論文95-32A-8-18

4x4 매트릭스 광스위치의 최적 설계

(An Optimal Design of 4x4 Optical Matrix Switch)

崔 原 準 *, 洪 聖 喆 **, 李 錫 *, 金 會 宗 *, 李 精 一 *, 姜 光 男 *, 曺 圭 晩 ***

(Won Jun Choi, Songcheol Hong, Seok Lee, Hwe Jong Kim, Jung Il Lee, Kwang Nham Kang, Kyuman Cho)

요 약

광손실의 측면에서 단순 트리구조를 갖는 GaAs/AlGaAs 매트릭스 광스위치의 최적 설계과정이 제시되었다. 도핑에 의한 광손실을 고려하여 1.3 μm의 파장에서 광손실이 0.537 dB/cm인 pin형 GaAs/AlGaAs 광도파로 기판이 설계되었다. 설계된 기판상의 rib형 광도파로를 사용하는 경우에 대해, 4x4 매트릭스 광스위치의 연결소자인 역 Δβ형 전기광학 스위치의 동작전압, 소자길이 및 각 연결소자간의 연결을 위한 광도파로의 굽곡손실이 광도파로 변수 및 곡률반경의 함수로 계산되었다. 광도파로 변수들 및 광도파로의 곡률반경을 고려하여 4x4 매트릭스 광스위치의 광손실을 계산한 결과, 일정한 광도파로 변수에 대해 광손실을 최소로 하는 최적의 광도파로 곡률반경이 존재한다. 공정에 둔감하고 적은 광손실을 갖는 4x4 매트릭스 광스위치의 제작을 위해서는 rib형 광도파로의 rib 높이 및 너비가 큰 등의 광구속이 큰 조건으로 광도파로를 제작해야 할 것으로 분석되었다. 이러한 분석에 근거하여 3 dB 광손실을 갖는 동작전압 12 volt의 4x4 매트릭스 광스위치가 설계되었다.

Abstract

The design procedure of a GaAs/AlGaAs semiconductor matrix optical switch is presented for a simplified tree architecture in the viewpoint of optical loss. A low loss, 0.537 dB/cm, pin type substrate is designed by considering the loss due to impurity doping at 1.3 μm wavelength. The operating voltage and the device length of a reversed Δβ electro-optic directional coupler(EODC) switch which is a cross-point device of the 4x4 matrix optical switch and the bending loss of rib waveguide are caculated as functions of waveguide parameters and bending parameters. There is an optimum bending radius for some waveguide parameters. It is recommened that higher optical confinement conditions such as wide waveguide width and higher rib-height should be chosen for structural parameters of a low loss and a process insensitive 4x4 matrix optical switch. A 4x4 optical matrix switch which has a 3 dB loss and a 12 volt operating voltage is designed.

* 韓國科學技術研究院 情報電子 研究部
(Division of Elec. and Infor. Tech., KIST)
** 正會員, 韓國科學技術院 電氣 및 電子工學科
((Dept. of Elec. Eng., KAIST)
*** 正會員, 西江大學校 物理學科
(Dept. of Physics, Sogang Univ.)
接受日字:1995年 2月 21日, 수정완료일:1995年 7月 29日

I. Introduction

There is an increasing demand for optical fiber communications, which make broadband communication networks possible. With its wide bandwidth, especially near the wavelength 1.3 μm and/or 1.5 μm, optical fiber communications can adopt various communication techniques such as space division, time division and wavelength division multiplexing techniques, which are thought to be key techniques for the realization of broadband integrated service digital networks. Integrated waveguide optical switches are thought to be key elements for the development of such technology. There have been considerable efforts to make such integrated waveguide optical switches on $LiNbO_3$ substrate[1-3]. Though $LiNbO_3$ waveguide optical switches have some atractive features such as low propagation loss and low switching power because of its high electrooptic coefficient, there is no possibility of its integration with high speed electronic circuits and active devices such as laser diode, photodetector, and optical amplifier which are made on III-V compound semiconductors such as GaAs and InP. Therefore much efforts have been concentrated on the fabrication of the III-V semiconductor waveguide[4] and related optical switches[5-10].

There are several kinds of semiconductor optical switches suitable for a matrix optical switch, such as a carrier injection type[5,6], a total internal reflection type[7], a gain guided type[8], and a directional coupler type[9-11]. A reversed $\Delta\beta$ type electrooptic directional coupler(EODC) is thought be suited for a unit device of matrix switch, because its high speed operation, low electric power consumption, and little indepdence of input carrier wavelength. The characteristics of an EODC is much dependent on the variations due to device fabrication[10]. Since the epitaxial layer growth techniques of GaAs/AlGaAs semiconductor and the GaAs-based device fabrication techniques are mature, it is better to choose the GaAs-based epitaxial structure as the substrate for an EODC matrix optical switch.

To get an optimum design for a GaAs/AlGaAs 4x4 matrix switch in the viewpoint of optical loss, it is desired to consider the loss due to a doping concentration of each epitaxial layer, waveguide bending loss, and scattering loss. Because the scattering loss is dependent on the fabrication processes, it is difficult to consider the scattering loss in the design of the switch. The waveguide bending loss is dependent on the dimensions of waveguide and bending radius. Moreover, the switching voltage of an EODC is a function of waveguide dimensions[10]. Therefore it is desirable to analyse the waveguide including loss. A transfer matrix method(TMM)[11] is used to analyse the GaAs/AlGaAs multiple waveguide. This method can treat not only the multiple layer structure including metal electrode but also the loss due to its doping concentration.

There are many structural parameters to be considered in the design of the 4x4 matrix optical switch such as waveguide parameters, EODC's parameters, and bending parameters. They are closely related to each other. One have to consider all these parameters to design a low loss 4x4 matrix optical switch. A low loss substrate design is essential to accomplish this purpose. This is illustrated in section II. In section III, bending loss dependence on the structural parameters such as waveguide parameters and bending parameters, is described. A cross-point device, reversed $\Delta\beta$ EODC switch determines many of

the chracteristics of matrix optical switches. In section IV, The chracteristics of this type of switch, such as switching voltage and device length, and their dependences on the structural parameters of EODC are described. Using the analysis of its loss dependence on the structural parameters, an optimal design of the 4x4 matrix switch is dicussed in section V. Summary is presented in section VI.

Ⅱ. Substrate design

It is desired for the device to have a low operating voltage. For this purpose, the guiding region of the waveguide should be thin. In this configuration, a pin type substrate structure is favorable because, for a constant external bias voltage, a higher electric field in the intrinsic layer can be obtained by reducing the thickness of the intrinsic layer. The switching voltage of the EODC switch is closely related to the overlap between the electric field and the optical field. The optical loss is also a function of confinement factor. Therefore it is important that the optical wave should be highly confined in the intrinsic region of the pin type substrate.

The real part of the dielectric constant of a III-V compound semiconductor is given [13] as

$$\varepsilon_1 = A\left\{f(\chi)+\frac{1}{2}\left[\frac{E_0}{(E_0+\Delta_0)}\right]^{3/2} f(\chi_{so})\right\} + B \quad (1)$$

$$, \chi = \hbar\omega/E_0$$

$$, \chi_{so} = \hbar\omega/(E_0+\Delta_0)$$

$$, f(x) = x^{-2}\{2-(1+x)^{1/2}-(1-x)^{1/2}\}$$

,where ω is angular frequency of the optical wave, and other parameters given for $Al_xGa_{1-x}As$ semiconductor, as a function of Al mole fraction, x, are as follows.

$$E_0(x) = 1.425+1.155x+0.37x^2 \quad (2)$$

$$\Delta_0 = 1.765+1.115x-0.37^2 \quad (3)$$

$$A(x) = 6.3+19.0x \quad (4)$$

$$B(x) = 9.4-10.2x \quad (5)$$

The refractive index of $Al_xGa_{1-x}As$ can be expressed as

$$n(x,\omega) = \varepsilon_{1(x,\omega)}^{1/2}. \quad (6)$$

The maximum thickness of the GaAs guiding layer for the fundamental mode can be calculated for the 3 layer waveguide whose cladding layer is $Al_xGa_{1-x}As$ [14]. Fig. 1 shows the cutoff thickness of GaAs guiding layer as a function of the Al mole fraction x for a TE0 mode of 1.3 μm wavelength. For the doped semiconductor, there is a reduction in its refractive index and increase in its absorption. Such changes have been explained by free carrier effect [14], and expressed as

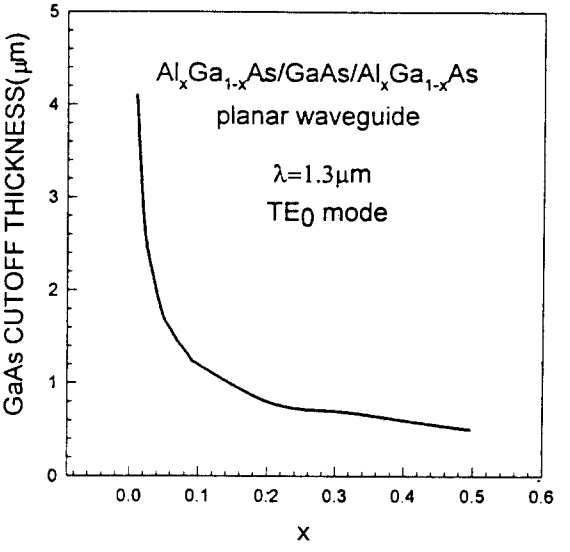

그림 1. $Al_xGa_{1-x}As/GaAs/Al_xGa_{1-x}As$ 평판 도파로에서 1.3 μm 파장의 TE_0 모드를 허용하는 GaAs 도파층의 Al mole fraction에 따른 허용두께

Fig. 1. Cutoff thickness of GaAs guiding layer of $Al_xGa_{1-x}As/GaAs/Al_xGa_{1-x}As$ planar waveguide for 1.3 μm wavelength TE_0 mode.

$$\Delta n = -\frac{Ne^2}{2n_0\varepsilon_0 m^* \omega^2} \quad (7)$$

and $$\alpha = \frac{Ne^3\lambda^3}{4\pi n_0 m^{*2}\mu\varepsilon_0 c_0^3} \quad (8)$$

, where Δn is index change, α is absorption coefficient, N is doping concentration, e is electronic charge, n_0 is refractive index, ε_0 is permittivity of vacuum, m^* is effective mass of free carrier, μ is mobility of free carrier, and c_0 is speed of light in vacuum. The complex refractive index is expressed as

$$n = n_r + in_i \quad (9)$$

,where n_r is the real part of the refractive index and n_i is the imaginary part of refractive index which is related to the absorption and/or the gain in the waveguide. For the lossy medium, n_i is termed as extinction coefficient and is a negative value. The extinction coefficient is expressed in terms of absorption coefficient as

$$\alpha = -\frac{4\pi n_i}{\lambda} \quad (10)$$

,where λ is optical wavelength. Since the refractive index and absorption coefficient(or extinction coefficient) can be calculated in the transparent wavelength region with the above equations, the complex refractive index of each epitaxial layer of a multiple layer waveguide can be obtained. After the calculation of complex refractive index of each layer, the effective refractive index of a GaAs/AlGaAs multiple layer waveguide can be obtained as a complex number through the TMM[11]. Since the imaginary part of effective refractive index is related to absorption coefficient as Equation (10), one can obtain a propagation loss for certain multiple layer waveguides.

In the viewpoint of the coupling between the waveguide and the optical fiber, thinner waveguide may cause higher coupling loss because of mode mismatch[15]. The fiber coupling loss is mainly dependent on the waveguide dimension. Though a wider and thicker waveguide reduces the coupling loss, it requires an EODC switch with a higher operating voltage[10]. The epitaxial layer structures of these two substrates are shown in Fig. 2. As shown in Fig. 2, this structure has intrinsic AlGaAs layers to minimize the optical loss due to its free carriers.

0.2 μm	p^+- GaAs (P^+=2E18/cm)
0.6 μm	p- $Al_{0.5}Ga_{0.5}As$ (p=3E17/cm^3)
0.3 μm	i- $Al_{0.5}Ga_{0.5}As$
0.3 μm	i- GaAs
0.2 μm	i- $Al_{0.5}Ga_{0.5}As$
1.5 μm	n- $Al_{0.5}Ga_{0.5}As$ (n=5E17/cm^3)
	n^+- GaAs (n^+=2E18/cm)

그림 2. 기판의 epi 구조
Fig. 2. Epi-layer structure of substrate.

The effective complex refractive index of structure is calculated with the TMM[11] at 1.3 μm wavelength. The substrate structure permits only a fundamental mode. Fig. 3 shows the mode intensity distribution, which exhibits a single mode characteristics. Propagation loss of 0.537 dB/cm is calculated. The fiber coupling loss is mainly dependent on the mode mismatch between the optical fiber and the channel waveguide[15]. The core diameter of a single mode optical fiber is about 9 μm at 1.3 μm wavelength. Though the maximum lateral size of semiconductor rib waveguide for a fundamental mode is a function of rib-height and its vertical structure, it is possible to choose the lateral

size as 2.5 μm with a moderate manner. With these parameters including the vertical structures of the two types of substrate, coupling loss of 11.98 dB is calculated. Though this structure has relatively high coupling loss, it would have small switching voltage because of its thin intrinsic layer.

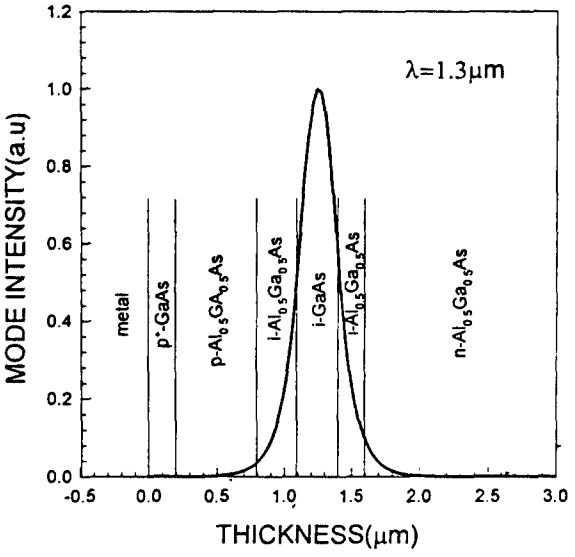

그림 3. 기판에서 1.3 μm 파장의 TE_0 모드 도파광에 대한 도파모드 세기분포
Fig. 3. Mode intensity distribution for 1.3 μm wavelength TE_0 mode.

Ⅲ. Design of rib waveguide and bending structure

Fig. 4 shows the schematic diagram of a rib waveguide. The rib-height, D is controlled by an etching process. Since the effective refractive indices of region I, II, and III can be calculated with the TMM as described before, the effective complex refractive index of rib waveguide can also be calculated with the TMM.

There is radiation loss in a waveguide bending structure. Such a radiation loss is a function of the bending structure, and the waveguide parameters. The attenuation coefficient of the radiation loss due to its S-shaped bending structure is given[16] by

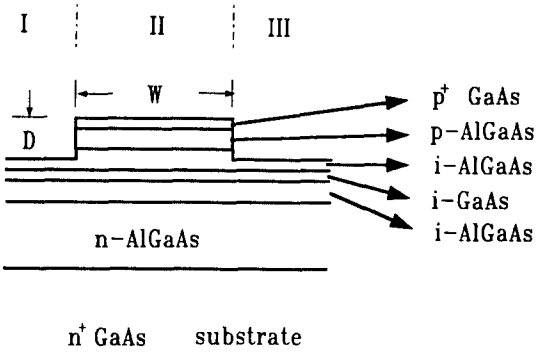

그림 4. Rib 광도파로의 개략도
Fig. 4. Schematic diagram of rib waveguide.

$$\alpha_r = \frac{\frac{1}{2q}\cos^2(pW/2)\exp\left(-2q\frac{\beta_{II}-\beta_I}{\beta_I}R\right)2\lambda\exp(qW)}{\left\{\frac{W}{2}+\frac{1}{2p}\sin(pW)+\frac{1}{q}\cos^2(pW/2)\right\}W^2} \quad (11)$$

$$q^2 = (N_{eff}^2 - n_1^2)\,k_0^2 \quad (12)$$

$$p^2 = (n_{II}^2 - N_{eff}^2)\,k_0^2 \quad (13)$$

$$\beta_I = n_I\,k_0 \quad (14)$$

$$\beta_{II} = N_{eff}\,k_0 \quad (15)$$

,where k_0 is wavenumber in vacuum, W is waveguide width, R is bending radius, β_I and β_{II} are propagation constants in region I and in region II, respectively. As seen in Equation (11), the bending loss depends exponentally on the bending radius and on the waveguide parameters such as waveguide width, rib-height, and its vertical structure.

Fig. 5 shows a schematic diagram of the S-shaped bending structure. After a simple calculation, one can obtain the total path length in the curvature, L_{cr} and length L as a function of bending parameters, when bend offset T is smaller than bending radius R, as

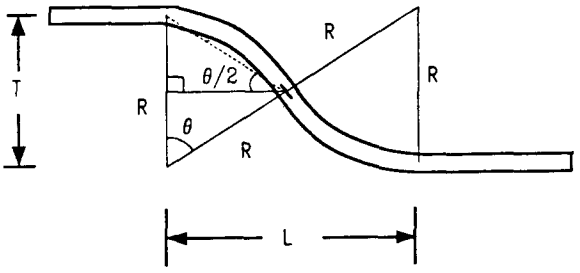

그림 5. S자형 굴곡구조의 개략도
Fig. 5. Schematic diagram of S-shaped bending structure.

$$L_{cl} = 4R\sin^{-1}\left(\frac{1}{2}\sqrt{\frac{T}{R}}\right) \quad (16)$$

$$L = 2\sqrt{R^2-(R-T/2)^2} \quad (17)$$

Since the waveguide parameters should be determined in accordance with the characteristics of the EODC switch, the bending loss is mainly dependent on the bending radius. For the constant waveguide parameters, bending loss can be calculated.

Fig. 6 shows the dependence of the bending loss of an S-shaped bending structure on the waveguide parameters for T=100 μm. The bending loss exponentially decreases as the bending radius increses. The bending loss decreases with the waveguide width, as seen in Fig. 6-(a). Therefore the waveguide width should be as wide as the cutoff width of the fundamental mode, in the viewpoint of the bending loss. As seen in Fig. 6-(b), the bending loss also decreases with the rib-height. These indicate, that higher confinment condition results in lower bending loss.

One may conclude that, only for the bending structure, larger bending radius, wider wavguide width, and deep etching in a rib waveguide fabrication results in low bending loss. However, this conclusion may lose its validity in the whole design of 4x4 matrix optical switch, because the characteristics of the EODC switch, such as switching voltage and coupling length are dependent on the waveguide parameters. Therefore such parameters should be determined in accordance with the design of the EODC switch.

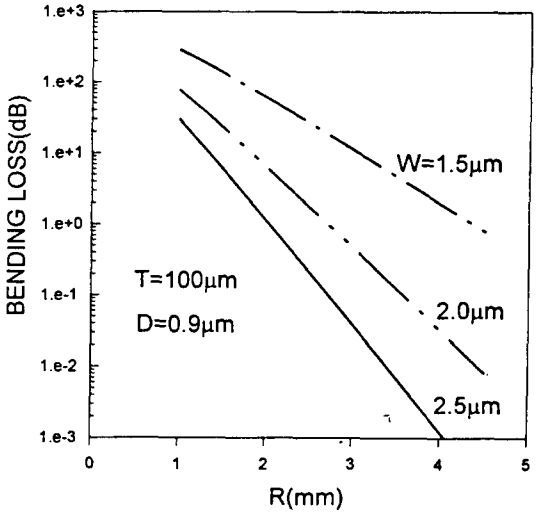

(a)

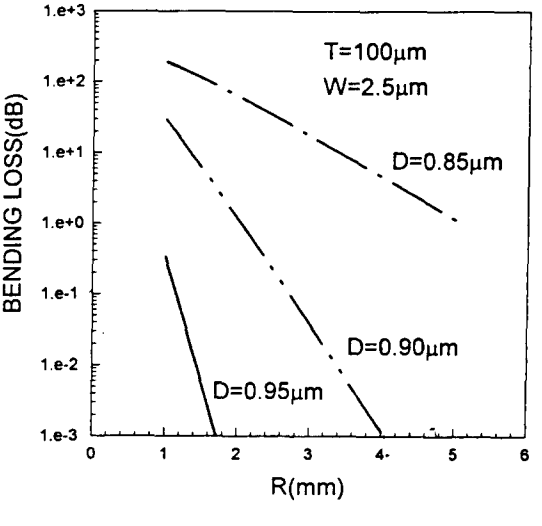

(b)

그림 6. S자형 굴곡구조의 (a) W 및 (b) D에 대한 굴곡손실
Fig. 6. Bending loss of S-shaped bending structure with respect to (a) W and (b) D.

Ⅳ. Design of reversed Δβ type EODC switch.

Fig. 7 shows the schematic diagram of reversed Δβ type EODC switch. The conditions for a cross(⊗) state and for a bar(⊖) state are expressed[17], respectively, as

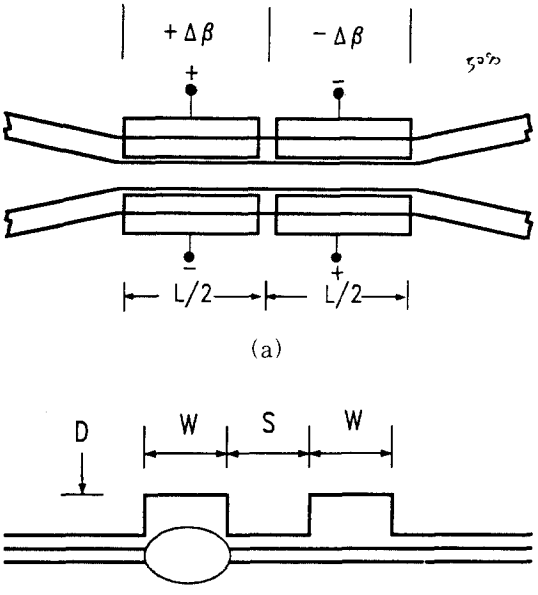

그림 7. (a) 역 Δβ형 EODC 스위치 및 (b) 단면도

Fig. 7. Schematic diagram of (a) reversed Δβ type EODC switch and (b) its crossectional view.

$$\frac{x^2}{x^2+\delta^2}\sin^2\left(\frac{L}{2}\sqrt{x^2+\delta^2}\right) = \frac{1}{2} \tag{18}$$

$$\left(\frac{L}{l_0}\right)^2+\left(\frac{\Delta\beta L}{\pi}\right)^2 = (4\nu)^2 \tag{19}$$

, where

$$\Delta\beta = \frac{1}{2}k_0 n^3 r\frac{V}{d} \tag{20}$$

$$l_0 = \frac{\pi}{2x} \tag{21}$$

$$L = \eta l_0. \tag{22}$$

x is coupling constant of EODC, L is device length of EODC, l_0 is coupling length of EODC, ν is an integer, $\delta(=\Delta\beta/2)$ is mismatch, r is electrooptic coefficient (=1.6x10-12m/V[18]) of GaAs and/or AlGaAs, n is refractive index of GaAs and/or AlGaAs, V is applied voltage, and d is thickness of intrinsic layer of the substrate. By assuming that the overlap integral between light field and applied electric field is a unit, ⊖ state switching voltage can be calculated, for $\nu = 1$ and $L = \eta l_0$, from the Equation (19) and (20), as

$$V_{\ominus} = \frac{4\sqrt{16-\eta^2}xd}{\eta n^3 r k_0}. \tag{23}$$

For $\delta^2 = \eta^2 x^2$, Equation (18) can be expressed as

$$\frac{1}{1+\xi^2}\sin^2\left(\frac{\eta\pi}{4}\sqrt{1+\xi^2}\right) = \frac{1}{2}. \tag{24}$$

Therefore ⊗ state voltage is expressed as

$$V_{\otimes} = \frac{4\xi xd}{n^3 r k_0} \tag{25}$$

, when ξ satifies Equation (24). One can calculate ξ numerically as a function of η. Since the coupling constant x, is given[14] as

$$x = \frac{2q^2 p\exp(-pS)}{\beta(q^2+p^2)(W+2/p)} \tag{26}$$

, one can calculate the coupling length, bar state voltage and cross state voltage as a function of the geometrical parameters of the EODC.

The switching voltage and the device length of a reversed Δβ type EODC switch are shown in Fig. 8. The switching voltage decreases exponentially with the separation between the waveguides. Since the device length of a reversed Δβ type EODC switch is inversely proportional to switching voltages, as seen in Equation (21), (22), (23), and (25), it exponentially increases with the separation of the waveguides. Since the switching voltage is proportional to η, it increase with η and the device length decreases. One can see other

structural dependences of the switching voltage and device length in Fig. 8-(a) and (b). The switching voltage decreases with the waveguide width and the rib-height.

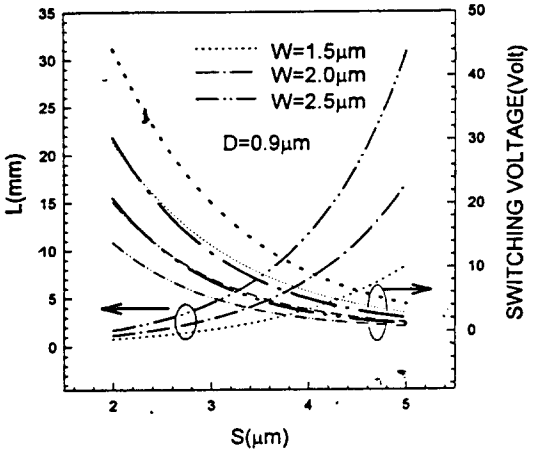

(a)

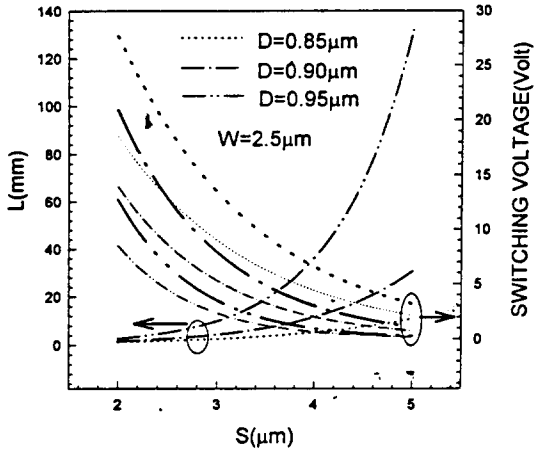

(b)

그림 8. 역 Δβ형 EODC 스위치의 (a) W 및 (b) D에 대한 스위칭 전압 및 소자 길이. 굵은 선은 ⊗ 상태의 스위칭전압을 가는 선은 ⊖ 상태의 스위칭전압을 나타낸다.

Fig. 8. The switching voltage and the device length of reversed Δβ type EODC switch with respect to (a) W and (b) D. Thick lines represent ⊗ state voltages and thin lines represent ⊖ state voltages.

The device length increases with the waveguide width and the rib-height.

Since the bending loss decreases with the waveguide width and the rib-height, one may conclude that wider waveguide width and larger rib-height result in lower loss in a 4x4 matrix optical switch. However, since wider waveguide width and larger rib-height require longer device length, these conditions result in higher propagation loss. Since the breakdown voltage of the substrate and a real propagation loss including scattering loss depend on substrate characteristics and device fabrication techniques, it might be feasible to determine the characteristics of the reversed Δβ EODC switch such as switching voltage, which can be determined by the structural parameters. After determining the structural parameters, one can find an optimum condition by reducing the losses due to passive parts of 4x4 matrix optical switch. These losses are closely related to the architecture of the 4x4 matrix optical switch.

V. Design of 4x4 matrix optical switch

Since 4x4 matrix optical switches have many cross-point devices and bending structures to connect cross-point devices, its architecture affects the loss and the cross talk between the output ports. There are several kinds of matrix switch architecture such as cross bar, tree, and simplified tree architecture[19,20]. As pointed out by K. Komatsu et al.[11], the simplified tree architecture have adventages of smaller path depenedance in propagation loss, a small number of unit cross devices and bending structures, and low cross talk level. Therefore it is feasible to adopt the simplified tree architecture as an architecture for the 4x4

matrix optical switch.

Fig. 9 shows the 4x4 matrix optical switch whose architecture is the simplified tree architecture. This architecture has 12 EODCs and numerous waveguide bends. As illustrated above, one can calculate all the bending parameters such as the optical path length in bending structure and its longitudinal length, as a function of its bending radius, R and its bend offset, T. Since the smaller bend offset results in lower bending loss, small bend offset is feasible to design low loss matrix optical switch. In practice, considering the coupling between the waveguide and the optical fiber which is mounted on V-grooved Si substrate, one can get the smallest bend offset of 100μm[21] to maintain the length between the adjacent ports as same.

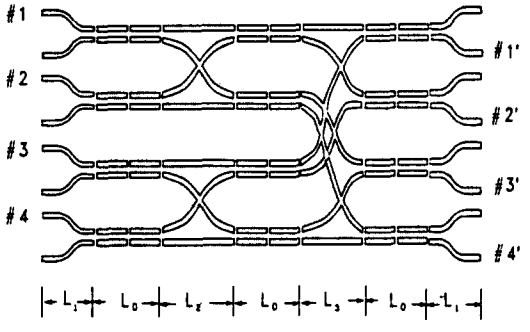

그림 9. 4x4 매트릭스 광스위치의 단순 트리 구조의 개략도

Fig. 9. A simplified tree architecture of 4x4 matrix optical switch.

As seen in Fig. 9, the 4x4 matrix optical switch has 4 kinds of waveguide bend, whose bend offsets are different from each other. If one makes the radii of these waveguide bends large in order to reduce this bending loss, the total loss will increase because the larger bending radius cause the longer optical path length and results in higher propagation loss. Though these different bend offsets have different bending losses, the differences of bending loss are negligible for large R. Therefore it is feasible to adopt equal R for these waveguide bends.

The total device length is expressed as,

$$L_{tot} = 3L_0+2L_1+L_2+L_3 \quad (27)$$

,where L_0 is a device length of EODC switch. L_1, L_2, and L_3 can be calculated by Equation (17). The optical path length for each bend can also be calculated by Equation (16). The total device length and the total optical path length are functions of R. Therefore, it is simple to calculate the total loss for each optical path, including propagation loss and bending loss as a function of R. The optical path from input port #1 to output port #4′ results in the maximum loss for the constant device parameters including waveguide parameters and bending radius. One should minimize this loss in order to design low loss 4x4 matrix optical switch.

The total loss and the total device length are shown in Fig. 10 as a function of R for T=100 μm. It is noted that there is an optimum bending radius, R for the constant waveguide parameters and the sepearation between the waveguides of EODC. This optimum R is determined by the waveguide parameters such as W and D.

For smaller radius than the optimum R, the total loss depends mainly on the bending loss. However, for larger radius than the optimum R, since the total loss depend mainly on the propagation loss, the increasing ratios of the total loss is equal for all data in Fig. 10. As for a loss difference between the loss due to the optical path from #1 port to #4′ port and the loss due to the optical path from #1 port to #1′ port, this loss difference is at most 0.1 dB for larger radius than the optimum R.

Though the propagation loss of the substrate used in this calculation is 0.537 dB/cm, there must be a additional loss mainly due to scattering loss. This additional loss is smaller than 1 dB/cm[22]. Even considering an 1 dB/cm additional loss, the optimum R value is not changed.

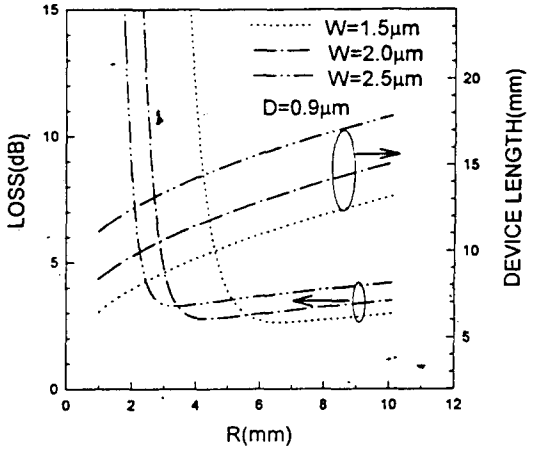

(a)

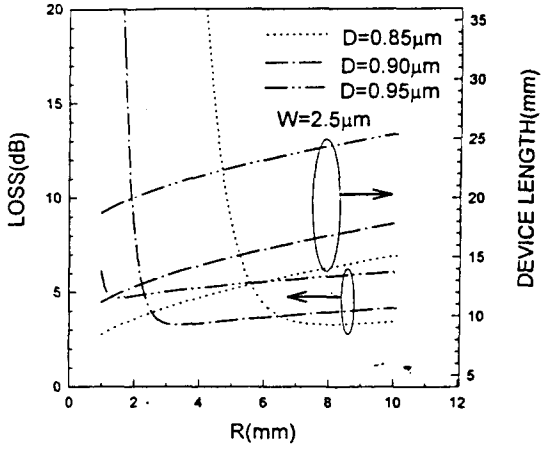

(b)

그림 10. T=100 μm, η=1.5 및 S=2.5 μm 일 때 (a) W 및 (b) D에 대한 총 손실 및 4x4 매트릭스 광스위치의 소자길이

Fig. 10. The total loss and the device length of 4x4 matrix optical switch with respect to (a) W and (b) D for T=100 μm, η=1.5, and S=2.5 μm.

Therefore one can find this optimum bend radius in order to design low loss matrix optical switch regardless of additional loss.

It is recommendable to design a low loss matrix optical switch that the waveguide parameters should be determined in accordance with the requirement of the switching voltage of the reversed Δβ EODC switch, within the permission of a substrate breakdown voltage. After the design of the reversed Δβ EODC switch, an optimum bending radius can be found easily. One should also consider the tolerences which should be accompanied during the device process such as lithograghy and etching process because these tolences may deteriorate the performances of matrix optical switch.

If these tolerences make the waveguide width and the rib-height larger than their designed value, there will be a little increase in the total loss of the matrix optical switch for the optimum R determined by the designed value, as seen in Fig. 10-(a) and (b). However, in practice, there are many possibilities for waveguide parameters to be smaller than their designed value, especially in the process of photolithograpy for a long device. In this case, there must be a considerable increasing of the total loss. Therefore it is recommendable, to reduce such possiblities of drastic increasing of the total loss, that the waveguide parameters such as waveguide width W and rib-height D should be as large as the value permitted by the fundamental mode cutoff condition. It is also recommendable that bending radius R should be larger than the optimum value which is determined by the waveguide parameters. With such design rules, a matrix optical switch which has low switching voltage and low total loss can be made with a process tolerent manner.

According to the above design rule, one can design a waveguide whose waveguide width W and rib-height D are 2.5 μm and 0.9 μm, respectively. The separation between the waveguides of EODC, S can be chosen to be a 2.5 μm, which results in V⊗=8.6 volts and V⊖=12.9 volts for η=1.5. In this case, the total loss is about 3 dB and the device length is about 14 mm for bend offset T=100 μm as seen in Fig. 11-(c) and (d).

Ⅵ. Summary

A loss pin type GaAs/AlGaAs hetero-structure substrate is designed for a 4x4 matrix optical switch. The analsis of this structure is carried out with the TMM. This substrate has a 0.537 dB/cm loss at 1.3 μm wavelength TE0 mode light when considering only a free carrier effect.

The relation between the parameters of a S-shaped rib waveguide bending structure such as bending radius, its bend offset and its longitudinal length is presented. The waveguide bending loss is calculated as functions of bending radius and its waveguide parameters such as waveguide width and rib height, in conjunction with the analysis of a rib waveguide through the TMM. The bending loss decreases exponentially with the bending radius. The bending loss also decreases for higher confinement conditions such as wide waveguide width and large rib-height. For the constant bending radius and waveguide parameters, the bending loss increases with bend offset because of its optical path length.

A reversed Δβ type EODC switch is adopted as a cross-point device for the 4x4 matrix optical switch. The analysis of this switch is carried out by a coupled mode theory in conjunction with the TMM. A coupling length and a switching voltage are calculated as functions of waveguide parameters, a separation between the waveguides of EODC, and η. The coupling length of EODC increases exponentially with the separation between the waveguides of EODC. The coupling length also increases with higher confinement conditions such as wider waveguide width and larger rib-height. The switching voltage of the reversed Δβ type EODC switch is decreases exponentially with the separation of waveguides of EODC. The switching voltage also decreases with higher confinement conditions. The smaller length parameter η results in the higher switching voltage because of its shorter device length.

A simplified tree architecture is adopted for a architecture of the 4x4 matrix switch. The loss and the device length of the 4x4 martrix optical switch are calculated as functions of waveguide parameters and bending parameters. There is an optimum waveguide bending radius for some waveguide parameters and EODC's parameters. Therefore one should find an optimum bending radius to design a low loss 4x4 matrix optical switch when the switching voltage of cross-point device, the reversed Δβ EODC switch is determined by waveguide parameters in accordance with the substrate breakdown voltage. Considering the process tolerences, it is recommended that higher optical confinement conditions such as wide waveguide width and higher rib-height should chosen for a low loss and a process insensitive 4x4 matrix optical switch. With such a design rule, a 14-mm long 4x4 matrix optical switch which has a 3 dB loss and a 12 volt operating voltage is designed.

References

[1] J. Erickson, G. Bogert, R. Huisman, and R. Spanke, "Performance of Two

4x4 Guided-Wave Photonic Switching Systems", *IEEE J. Sel. Areas. Commun.*, Vol. SAC-6, no. 12, pp. 1255, Aug. 1988.

[2] S. Suzuki, et al., "HDTV Photonic Space-Division Switching System using 8x8 Polaization Independent LiNbO3 Matrix Switch", Proc. Photonic Switching, pp. 168, Salt Lake, 1989.

[3] P. J. Duthie, M. J. Wale, and I. Bennion, "Size, Transparency and Control in Optical Space Switch Fabrics : A 16x16 Single Chip Array in Lithium Niobate and its Applications", Proc. Photonic Switching pp. 32, Kobe, Apirl 1990.

[4] H. Takeuchi, and K. Oe, "Low-Loss Single-Mode GaAs/AlGaAs Miniature Optical Waveguides with Straight and Bending Structures", *IEEE J. Lightwave Technol.*, vol. LT-7, no. 7, pp. 1044-1054, Jul 1989.

[5] Y. Okada, R. Yan, L. A. Coldren, J. L. Mertz, and K. Tada, "The Effect of Band-Tails on the Design of GaAs/AlGaAs Bipolar Transistor Carrier-Injected Optical Modulator/ Switch", *IEEE J. Quantum Electron.*, vol. QE-25, no. 4, pp.713-719, Apirl 1989.

[6] K. Ishida, H. Nakamura, H. Matsumura, T. Kadoi, and H. Inoue, "InGaAsP/InP optical Switches Using Carrier Induced refractive Index Change", Appl. Phys. Lett., vol. 50, pp. 141, 1987.

[7] T. C. Huang, T. Hausken, K. Lee, N. Dagli, L. A. Coldren, and D. R. Myers, "Depletion Edge Translation Waveguide Crossing Optical Switch", *IEEE Photonics Technol. Lett.*, vol. 1, no. 7, pp. 168-170, July 1989.

[8] D. K. Probst, L. G. Perrymore, B. C. Johnson, R. J. Blackwell, J. A. Priest, and C. L. Balestra, "Demonstration of an Integrated, Active 4x4 Photonic Crossbar", *IEEE Photonics Technol. Lett.*, vol. 4, no. 10, pp. 1139-1141, Oct. 1992.

[9] K. Komatsu, M. Sugimoto, A. Ajisawa, and A. Suzuki, "Small Size, Low-Crosstalk GaAs/AlGaAs Electro-optic Directional Coupler Switches with Alternating $\Delta\beta$ for Long Wavelength Matrix Switches", Proc. Photonic Switching, pp. 177, Salt Lake, 1989.

[10] W. J. Choi, J. I. Lee, K. N. Kang, S. Hong, and K. Cho, "Analysis of GaAs Schottky Contact Traveling Wave Optical Coupler", *J. Kor. Phys. Soc.*, vol. 26 no. 6, pp. 658, Dec. 1993.

[11] K. Komatsu, K. Hamamoto, M. Sugimoto, A. Ajisawa, Y. Gohga, and A. Suzuki, "4x4 GaAs/AlGaAs Optical Matrix Switches with Uniform Device Characteristics Using Alternating $\Delta\beta$ Electrooptic Guided-Wave Directional Couplers", *IEEE J. Lightwave Technol.*, vol. LT-9, no. 7, pp. 871-878, July 1991.

[12] K.-H. Schlereth, and M. Tacke, "The complex propagation Constant of Multilayer Waveguide: An Algorithm for a Personal Computer", *IEEE J. Quantum Electron.*, vol. QE-26, no. 4, pp. 627-630, Apirl 1990.

[13] S. Adachi, "GaAs, AlAs, and AlxGa1-xAs: Material parameters for use in research and device applications", *J. Appl. Phys.*, vol. 58 no. 3, pp. R1, Aug. 1985.

[14] R. G. Hunsperger, Integrated Optics: Theory and Technology, 2nd Ed, Springer-Verlag, p. 56, 1984.

[15] R. C. Alferness, V. R. Ramaswamy, S. K. Korotky, M. D. Divino, and L. L. Buhl, "Efficient Single-Mode Fiber to Titanium Diffused Lithium Niobate Waveguide Coupling for $\lambda = 1.32$ μm", *IEEE J. Quantum Electron.*, vol. QE-18 no. 10, pp. 1807, Oct. 1982.

[16] E. A. Marcacatili, "Bends in optical dielectric guides", *Bell Syst. Tech. J.*, vol. 48, pp. 2103-2132, 1969.

[17] H. Kogelnik, and R. V. Schmidt, "Switched Directional Couplers with Alternating Δβ", *IEEE J. Quantum Electron.*, vol. QE-12, pp. 396-401, 1976.

[18] S. Adachi and K. Oe, "Linear electro-optic effects in zincblende-type semiconductors: Key properties of InGaAsP relevant to device design", *J. Appl. Phys.*, vol. 56, no. 1, pp. 74, July 1984.

[19] P. Granestrand, B. Stoltz, L. Thylen, K. Bergvall, W. Doldissen, H. Heinrich, and D. Hoffman, "Strictly nonblocking 8x8 integrated optical switch matrix", Electron. Lett., vol. 22, pp. 816-818, 1986.

[20] I. Sawaki, T. Shimoe, H. Nakamoto, T. Iwama, Y. Yamane, and H. Nakajima, "An 8 mm Length Nonblocking 4x4 Optical Switch Array", *IEEE J. Sel. Areas. Commun.*, vol. SAC-6, no. 7, pp. 1267-1272, Aug. 1988.

[21] W. J. Choi, et al., Development of Optical Functional Devices Technology, Korea MOST Report No. UCN877-4614-4, 1992.

[22] H. Inoue, K. Himura, K. Ishida, T. Asai, and H. Matsumura, "Low Loss GaAs Optical Waveguides", *IEEE J. Lightwave Technol.*, vol. LT-3, no. 6,pp. 1270-1276, Dec. 1985.

저 자 소 개

崔 原 準(正會員)
1964년 2월 23일생. 1986년 2월 서강대학교 물리학과 졸업(이학사). 1988년 8월 서강대학교 대학원 물리학과 졸업(이학석사). 1989년 7월~현재 한국과학기술연구원 정보전자연구부연구원. 주관심분야는 광도파로형 광기능소자, 초고속 광변조기, tunable LD 및 OEIC등임.

李 錫(正會員) 第 32卷 1號 參照
현재 동경대 전자공학과 박사후 연수과정중

李 精 一(正會員) 第 26卷 5號 參照
현재 한국과학기술연구원 정보전자연구부 재직중

曺 圭 晩(正會員)
1954년 7월 31일생. 1978년 2월 서강대학교 물리학과 졸업(이학사). 1980년 2월 서강대학교 대학원 물리학과 졸업(이학석사). 1980년~1984년 공군사관학교 교수부 물리학과, 물리학 교관. 1994년~1991년 University of Marlyand 이학박사. 1991년~1992년 조교수. 주관심 분야는 고분해능 간섭식 센서를 이용한 변위, 전기장 및 자기장 센서의 개발, 고 분해능 표면구조 분석기 및 material mapper의 개발. 광통신소자 및 광통신 algorithm등임.

洪 聖 喆(正會員) 第 29卷 7號 參照
현재 한국과학기술원 전기 및 전자공학과 부교수

金 會 宗(正會員) 第 32卷 1號 參照
현재 한국과학기술연구원 정보전자연구부 재직중

姜 光 男(正會員) 第 26卷 5號 參照
현재 한국과학기술연구원 정보전자연구부 재직중